Electron Stimulation of Internal Torsion of a Surface-Mounted Molecular Rotor

Weihua Wang,[†] Xingqiang Shi,[‡] Mochen Jin,[†] Christian Minot,[‡,§] Michel A. Van Hove,[‡] Jean-Paul Collin,[⊥] and Nian Lin*,[†]

[†]Department of Physics, The Hong Kong University of Science and Technology, Hong Kong, China, [‡]Department of Physics and Materials Science, City University of Hong Kong, Hong Kong, China, [§]Laboratoire de Chimie Théorique, Université Pierre and Marie Curie, Paris 6, CNRS, UMR7616, Case 137, 4 Place Jussieu, Paris, F-75252 Cedex France, and [⊥]Institut de Chimie, Université Louis Pasteur-CNRS/UMR 7177, 4, Rue Blaise Pascal 67070 Strasbourg, France

ABSTRACT A molecular rotor which includes a central rotator group was investigated by scanning tunneling microscopy at 4.9 K as it was grafted on a Cu(111) surface *via* its two terminal groups. Topographs with submolecular resolution revealed several distinct molecular conformations which we attribute to different angular orientations of the rotator and which are locally stable states according to density functional theory calculations. Time-resolved tunneling current spectra showed that the rotator undergoes a torsional motion around the molecular long axis as stimulated by tunneling electrons in a one-electron process with an excitation energy threshold of 355 meV. Calculations identified an intrinsic axial vibration mode of the rotator group at 370 meV as adsorbed on the surface, which we propose to be the channel for effectively converting the tunneling electron energy into the mechanical energy of the intramolecular torsion.

KEYWORDS: Molecular rotor · electron excitation · scanning tunneling microscopy · density functional theory calculation

Molecular motions of artificial molecules are of great interest in the study of molecular machines and electronics.[1−9] In particular, surface-mounted molecules that move relative to the surface are regarded to have the best potential for applications, *e.g.*, for single-molecule electronic switches. It has been demonstrated that scanning tunneling microscopy (STM) is a powerful tool to address molecular motions on surfaces owing to its ability to directly reveal such motions by imaging different conformations with submolecular resolution. In addition, STM can manipulate or induce single molecular motions by tip−molecule interaction or electron tunneling, which provides a unique approach to investigate the mechanism of molecular motions.[10,11] To date, motions in which the molecules remain nearly rigid have been amply documented in the literature, including molecular rotations, vibrations, and lateral displacements.[12−29] However, large-angle intramolecular torsional motions (rotation or oscillation of a part of a molecule around a fixed molecular axle) have rarely been addressed experimentally even though such motions are fundamental to future molecular machinery.[1−5,30,31]

Here we report on a study of intramolecular torsional motions of an "altitudinal" rotor, defined as having its torsion axis parallel to the surface.[5] The chemical structure of the rotor molecule (4′,4′′′′-(bicyclo[2,2,2]octane-1,4-diyldi-4,1-phenylene)-bis- 2,2′:6′,2′′-terpyridine,[32] hereafter BTP-BCO) is shown in Figure 1a. It consists of two terminal terpyridine (tpy) groups acting as stands fixed to a substrate, a central bicyclo[2,2,2]octane (BCO) group acting as the rotator and two phenylene groups acting as a rotatable axle linking the rotator to the stands. As illustrated schematically in Figure 1b, the molecule is mounted on a Cu(111) surface, and the central rotator can undergo torsional motions around the axle when stimulated by tunneling electrons. The motions were monitored by STM topographs and time-resolved tunneling current spectra (tunneling current as a function of time, *I*-*t* spectra), which revealed several molecular conformations that can be attributed to distinctive axial angular states of the BCO group. These conformations were confirmed to be stable or metastable states by density functional theory (DFT) calculations. On account of the *I*-*t* spectra, the motions were found to be excited by one-electron processes, and an excitation energy threshold of 355 meV was derived. This value is close to the calculated energy of a torsional vibration mode (370 meV) of the BCO group as the molecule adsorbed on the surface in the most stable configuration. We propose that this vibration mode may effectively convert the tunneling electron energy into the mechanical energy of the intramolecular torsion.

*Address correspondence to phnlin@ust.hk.

Received for review June 13, 2010 and accepted July 14, 2010.

Published online July 21, 2010.
10.1021/nn101330c

© 2010 American Chemical Society

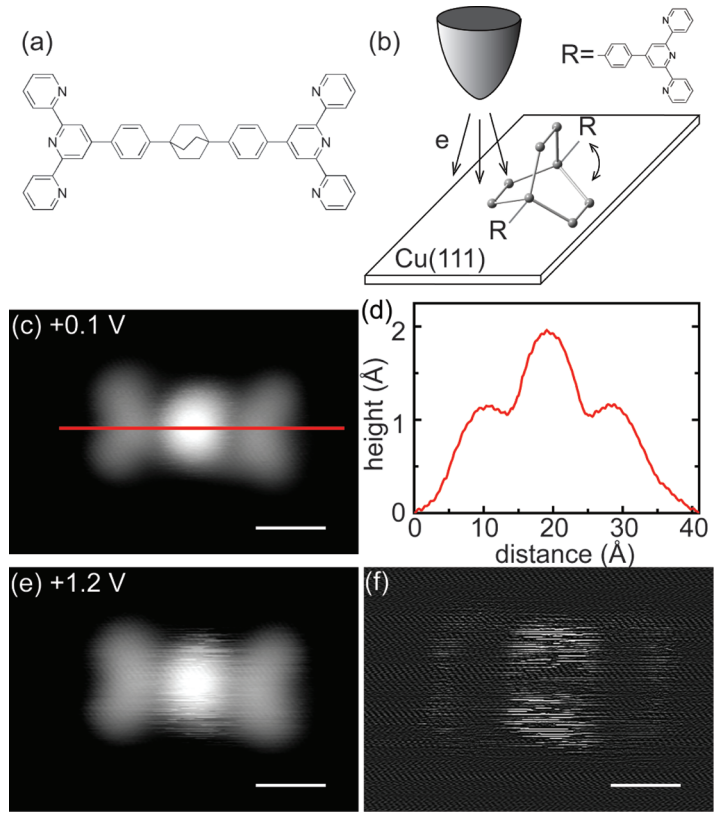

Figure 1. (a) Chemical structure of the BTP-BCO molecule. (b) Schematic of the stimulation of intramolecular torsional motion in the BTP-BCO molecule on the Cu(111) surface by tunneling electrons. (c) Representative STM topograph of a single BTP-BCO molecule acquired at low bias (V = 0.1 V and I = 0.5 nA). (d) A cross-sectional STM profile along the red line in c. (e) STM topograph of the same molecule acquired at high bias (V = 1.2 V and I = 0.5 nA). (f) Corresponding noise image of e. The scale bars in c, e, and f are 10 Å.

RESULTS AND DISCUSSION

Figure 1c represents a STM topograph of a single BTP-BCO molecule on Cu(111) acquired at a low sample bias voltage of 0.1 V, revealing the two tpy end groups and the central BCO group. A cross-sectional profile along the molecular long axis (Figure 1d) shows that the BCO group clearly protrudes above the tpy groups, by an apparent height difference of about 1 Å. This apparent value is much smaller than the actual height difference (in theory the height difference between nuclei is about 2.5 Å) due to the low density of states of the BCO at this imaging condition. At a higher sample bias, for example, 1.2 V as for Figure 1e, noisy spikes appeared in STM topographs, indicating that the tunneling current changes sharply. Figure 1f, a noise image (obtained by low-pass filtering the noise of Figure 1e), indicates that the noise is mostly localized at the BCO group, in particular near its edges, but not at the other parts of the molecule or at the clean Cu(111) surface. So we can exclude that the noise was caused by an unstable tip.

STM data have revealed that the single BTP-BCO topographs acquired at 0.1 V bias take three distinct shapes, as shown in Figure 2a−c, which we ascribe to three distinct molecular conformations. Figure 2a shows a symmetric conformation in which the BCO group is centered (denoted as C-state) on the molecular long axis, as indicated by the dashed line in Figure 2a. Figure 2b and c show two asymmetric conformations (mirroring each other) in which the BCO group is shifted either "southward" or "northward" (denoted as S- and N-states, respectively) relative to the molecular long axis (dashed lines in Figure 2b and c) in the topograph. The asymmetric molecular conformations are unambiguously displayed in the differential topographs shown as insets in Figure 2b and c. In addition to these distinctive static molecular conformations, the dynamic switching processes between the molecular conformations were probed by *I-t* spectra, positioning the tip over a specific site of the BCO group and applying a voltage pulse for a period of time with open feedback loop, while recording the tunneling current as a function of time. We found that the *I-t* spectra typically exhibit three levels: high (H), medium (M), and low (L), indicating three conductance states, as shown in Figure 2d−f.

To correlate the three molecular conformational states with the *I-t* spectra, we have carried out the following measurements: First an initial molecular state was recorded by acquiring a STM topograph at a low sample bias voltage of 0.1 V, which did not induce the motion (cf. Figure 2a). Then an *I-t* spectrum (for ex-

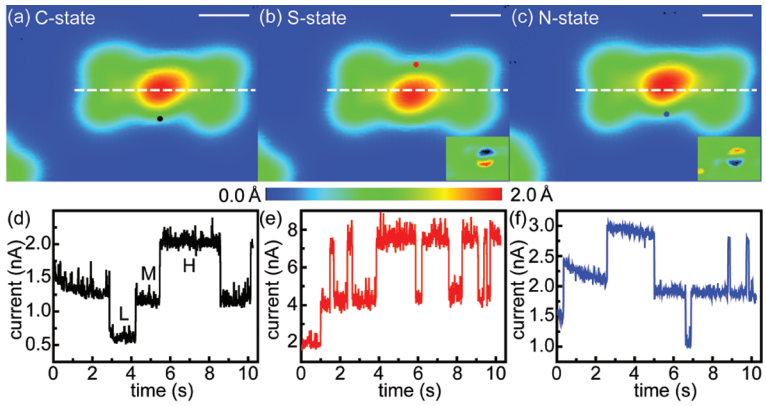

Figure 2. (a−c) Three STM topographs of the same BTP-BCO molecule scanned under the same conditions at a low bias showing three conformations C, S, and N, respectively (V = 0.1 V and I = 0.5 nA; the scale bar is 10 Å). Insets in b and c: Differential topographs of b−a and c−a. (d−f) I-t spectra recorded at the positions defined by black, red, or blue dots after acquiring the topographs a−c, respectively. (V = 0.35 V)

ample, Figure 2d) was recorded at a defined position (black dot in Figure 2a), typically for 10 s. Hereafter the same molecule was rescanned at 0.1 V to record its final state (cf. Figure 2b). This process was repeated many times on a single molecule under various conditions, *e.g.*, bias voltage, set tunneling current, and tip location. We found that, whenever the final conductance level of an I-t spectrum was different from its initial level, the molecular topographs showed different initial and final conformational states. For example, Figure 2d shows an initial conductance level M and a final level H, whereas the initial state is C (Figure 2a) and the final state is S (Figure 2b). By contrast, whenever the final conductance level of an I-t spectrum was the same as its initial level, the initial and final conformation states were always identical.

Furthermore, we identified a correlation between the initial conformational state and the subsequently acquired I-t spectra. For a C-state molecule (as in Figure 2a), the I-t spectra acquired at either the north or south side of the BCO group always start with the M level (as in Figure 2d). For a S-state molecule (as in Figure 2b), the I-t spectra acquired at the north side of its BCO group (red dot) always start with the L level (as in Figure 2e), while the I-t spectra acquired at the south side of its BCO group always start with the H level (not shown). For a N-state molecule (as in Figure 2c), the I-t spectra acquired at the north side of its BCO group always start with the H level (not shown), while the I-t spectra acquired at the south side of its BCO group (blue dot) always start with the L level (as in Figure 2f). A similar correlation was also observed between the final conductance level and the final conformational state, for example, as shown in Figure 2e and 2c.

To better understand the observed molecular conformations and the conductance behavior, we performed *ab initio* structure relaxations for the molecule adsorbed on a Cu(111) surface for various torsion angles of the BCO group, as illustrated in Figure 3a and b. First, the adsorbed molecule was fully relaxed in the "up" geometry, shown in Figure 3a, with the Cu(111) surface kept fixed. Next, the two tpy groups as well as the Cu surface were kept rigid, while the BCO group was rotated and then relaxed freely to find other potential local minima of the total energy (the tpy height above the metal was also reoptimized). Finally, we applied a third, complete reoptimization of the whole molecule, including the central BCO and the tpy groups, for each local minimum found for different BCO group rotations. Among all configurations, we found that three structures, named "up", "side", and "down", produce local minima of the total energy, as shown in Figure 3a. The up structure is the most stable, while the side and down structures are metastable, 0.24 and 0.37 eV higher in energy, respectively (the side structure is degenerate between equivalent right- and left-side structures). These energy differences are mainly caused by changes in three sets of interactions between the copper surface and the nearest hydrogen atoms (physisorption), the central BCO and the adjacent phenyl rings (intramolecular torsion and bending), and the phenyl rings and the terminal tpy groups (intramolecular bending). Table 1 summarizes the energy differences between the three configurations contributed by molecular conformation as well as by molecule surface adsorption.

The calculated height differences between the topmost carbon atom and the Cu(111) surface (kept flat) are given in Figure 3b, in which on-axis views of the BCO group are shown. In the up structure, a pair of carbon atoms of the BCO group points upward and is 5.49 Å above the Cu surface. In the side structure, the upper left pair of carbon atoms of the BCO group is 5.54 Å above the Cu surface, while the right pair of carbon atoms is 4.16 Å above the Cu surface. In the down structure, the two pairs of carbon atoms on either side of the BCO group are 5.30 Å above the Cu surface. Simulated STM topographs of the three configurations are shown in Figure 3c. In comparison with Figure 2, the main features of the experimental STM topographs are nicely reproduced by the simulations as either the sym-

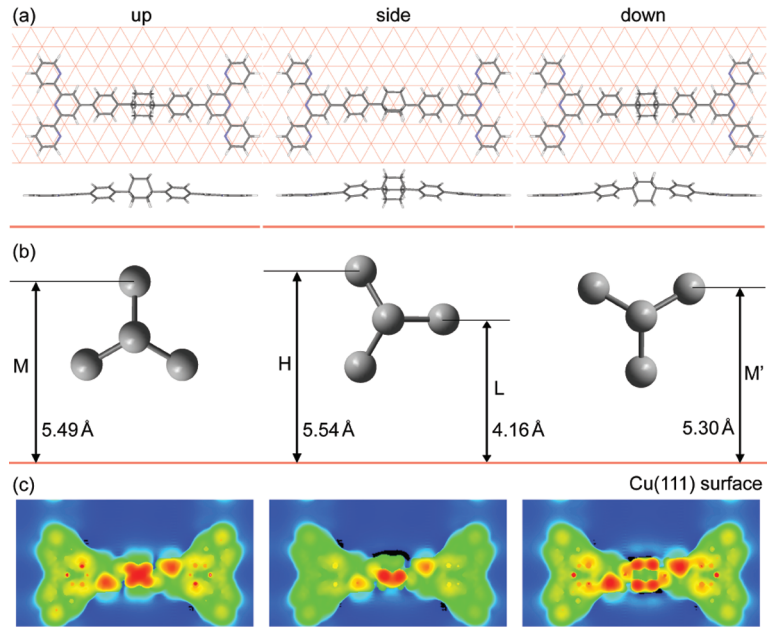

Figure 3. (a) Three calculated molecular conformations (top and side views) with locally minimum total energy, named up, side, and down structures from left to right, respectively. (b) On-axis cross-sectional views of the BCO group in the three respective structures of a (for clarity, H atoms are not shown); the calculated distances from the topmost carbon atom to the topmost Cu(111) nuclei are given. (c) Simulated STM topographs (33 × 18 Å) of the three conformations in a.

metrical up or down configurations are assigned to the C state and the asymmetrical right- or left-side configuration to the N or S states, respectively. On account of this assignment, the experimentally observed correlation between the *I-t* spectra and the conformational states can be rationalized as follows: When the tip was positioned over the left (right) side of the BCO group in the three structures of Figure 3b, the tip height over the nearest carbon atom was the smallest (largest) in the side structure and the intermediate in the up or down structures. For a molecule in the up or down conformation (left or right panel), the *I-t* spectra started with an M level current when the tip was over either the left or right side of the BCO group; for a molecule in the side conformation (central panel), the *I-t* spectra started with a H (L) level current when the tip was over the left (right) side of the BCO group.

Based on the foregoing discussion, we attribute the switching from one conformation to another to an intramolecular torsional rotation of the BCO group relative to the rest of the molecule, which remains largely immobile. In this molecule, the central BCO group is linked to the phenyl groups through C−C σ bonds. It is known that the C−C σ bond may easily undergo axial rotations. This rotation abruptly changed the separation between the tip apex atom and the nearest atoms of the BCO group, resulting in a jump of conductance in the *I-t* spectra.

TABLE 1. Energy Differences (in eV) between the Three Adsorption Configurations Due to Molecule−substrate Adsorption and Molecular Conformation Change[a]

configuration	up	side	down
adsorption energy	0.0	0.14	0.32
conformation energy	0.0	0.10	0.05

[a]Energies in the "up" geometry are used as references (energy zeroes).

Since the intramolecular torsional motions of the BCO group were monitored by the *I-t* spectra, we can extract further information from the tunneling current trace in the *I-t* spectra. The statistics of the residence time in each conformational state exhibit an exponential decay, from which a time constant may be derived. As this time constant directly reflects the molecule's residence time in a specific conformation, the inverse of the time constant defines the jumping rate from a certain conformation at the chosen sample bias and tunneling current. As an example, Figure 4a shows a distribution of states with residence time in the M level longer than the time given on the horizontal axis. The exponential decay fits a jumping rate from the M level of 1.55 ± 0.02 Hz. In Figure 4b, we plot the jumping rate from the M to the H or L levels as a function of tunneling current for four sample biases. The power-law fits of the data, $R \propto I^N$, give $N = 1.22 \pm 0.03$, 1.01 ± 0.23, 1.06 ± 0.03, and 1.04 ± 0.06 for sample biases of 0.25, 0.30, 0.35, and 0.40 V, respectively. The latter three values are close to unity, so we conclude that at the sample bias from 0.30 to 0.40 V the intramolecular torsional motions are stimulated by tunneling electrons in a one-electron process. At the sample bias of 0.25 V, a power of 1.22 hints that the multielectron processes may take place at this condition.

To quantify the stimulating energy threshold, we acquired the *I-t* spectra in a wide range of bias voltage. In Figure 4c, we plot the jumping rate from the M level as a function of sample bias.[13,15] It is clear that a drastic

increase of jumping rate appears at 355 ± 5 mV. This indicates that the threshold energy to stimulate the torsional motion is about 355 meV. This threshold energy is inconsistent with the results that at a low sample bias of 0.25 V, the multielectron processes occur since more than one electron is needed to stimulate the motion. At negative bias, the jumping rate from the M level shows a threshold energy near 355 meV as well. So, the electrons emitted from or injected into the tip stimulate the torsional motions equally. Our calculations reveal that as the molecule adsorb on the surface in the most stable (up) configuration, the BCO group vibrates around the molecular long axis with a mode of 370 meV. Since this energy is very close to the experimental threshold energy of the stimulation, we conjecture that this vibration mode may effectively assist the excitation of the intramolecular mechanical motion by the tunneling electrons.[13]

The noise image of Figure 1f highlights that the intramolecular torsional motions are very sensitive to the tip position. This sensitivity allows us to determine the most effective stimulation points. To that end, we recorded *I-t* spectra while positioning the tip at various points along a line perpendicular to the molecular long axis. We found that, at a fixed sample bias and tunneling current set point, the jumping rates between states M and H (M−H) or states M and L (M−L) exhibit a strong dependence on the tip position. Figure 4d shows the number of M−H and M−L jumping events per unit time as a function of tip position. The M−H jumping rate shows two maxima at the two edges of the BCO group and a local minimum in the center, while the M−L jumping rate shows a maximum in the center. At the two maxima, the M−H jumping rate is 10 times higher than the M−L jumping rate. Note that the molecular conformation that gives the H level current on one side gives the L level current on the other side, *i.e.*, M−H jumping on one side corresponds to M−L jumping on the opposite side. Thus when the tip was positioned on one side of the BCO group, the observed M−L jumping was actually the M−H jumping for the other side and *vice versa*. Therefore we can express the same molecular conformation change by the solid bell-shaped curves in Figure 4d. The curves imply that the molecular conformation changes have two stimulating centers located at both edges of the BCO group. When the tip was positioned at one stimulating center, it predominantly stimulated M−H jumping, and also M−L jumping with a much lower efficiency.

Finally, we point out that the calculated images reproduce symmetric-shaped STM topographs for both the up and down structures, but we cannot unambiguously determine which one is the experimentally observed C state. Nonetheless, since the up structure is 0.37 eV lower in energy, we assume that the up structure is the observed C state. It is worth noting that in our measurements we found a fourth conductance level in

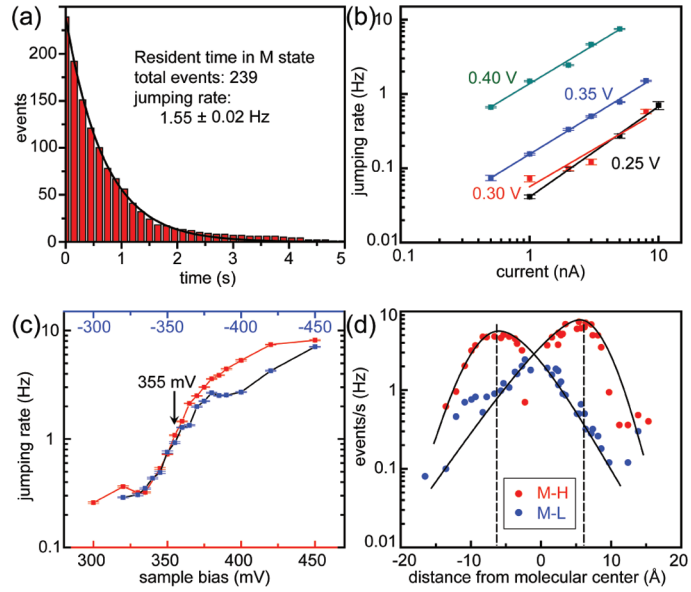

Figure 4. (a) Distribution of conformational states with residence time in the M level longer than the time given on the horizontal axis. The solid line is an exponential decay fit. The example given here is measured with a sample bias of 0.36 V and tunneling current set point of 4.0 nA. (b) Jumping rates from the M level as a function of tunneling current for four sample biases. The solid lines are the power-law fits to the data, $R \propto I^N$, where $N = 1.22 \pm 0.03$, 1.01 ± 0.23, 1.06 ± 0.03, and 1.04 ± 0.06 for sample biases of 0.25, 0.30, 0.35, and 0.40 V, respectively. (c) Jumping rate from the M level as a function of sample bias voltage with red (blue) curve corresponding positive (negative) bias voltage. It increases markedly at 355 ± 5 mV. (d) Number of M−H and M−L jumping events per unit time as a function of tip lateral distance from the molecular center. The tip was approximately positioned along the middle line perpendicular to the molecular long axis. The data were measured with a sample bias of 0.4 V. The solid lines relate molecular motions corresponding to the same molecular conformation change. The stimulating centers are indicated by dashed lines. The set point of the tunneling current is 4.0 nA for a, c, and d. The measuring time per point is 200−800 s for a and c and 100 s for d. The original *I-t* spectra were measured on the side of the BCO group for a−c.

the *I-t* spectra when the bias voltage is higher than 0.35 V. As shown in Figure 5a, another medium level, denoted as state M′, was observed. We propose that this M′ level probably corresponds to the down structure. Presumably because of its higher energy, this structure appears much less frequently than the two other structures. In Figure 5b, we plot each individual state of Figure 5a according to its current level. The arrows highlight the torsional motions between adjacent states, in which each red (blue) arrow indicates a 30° counterclockwise (clockwise) torsion. Clearly the BCO group undergoes torsional motions in both rotational directions randomly.

CONCLUSIONS

In conclusion, we have studied a single-molecule altitudinal rotor fixed on a surface. Stimulated by tunneling electrons, the central BCO group is found to undergo intramolecular torsional motions around the molecular long axis parallel to the surface. The motion was monitored by scanning tunneling microscopy (STM) topographs, which revealed several molecular conformations corresponding to distinctive torsional

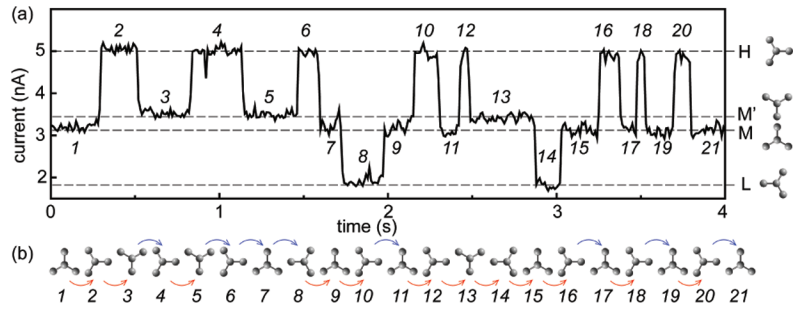

Figure 5. (a) A representative *I-t* spectrum that shows four conductance levels, where the two middle levels are denoted by M and M′ (sample bias: 0.38 V). (b) The BCO group conformation deduced for each individual state from the conductance level in a, where a red (blue) arrow indicates a 30° counterclockwise (clockwise) torsion between adjacent states. It is assumed that the M and M′ states correspond to the up and down BCO conformations, respectively (the tip is positioned over the left side of the BCO group in the measurements).

rotation states that were reproduced by density functional theory (DFT) calculations. On account of the *I-t* spectra, the motions were found to be excited by one-electron processes, and an excitation energy threshold of about 355 meV was derived, which is likely assisted by the 370 meV mode of the BCO group vibrating around the molecular long axis at its most stable adsorption configuration.

METHODS

The experiments were carried out in an ultrahigh vacuum scanning tunneling microscope (Omicron) operated at 4.9 K. The molecules (in powder form) were evaporated from a molecular beam evaporator (DODECON nanotechnology GmbH) and deposited onto a clean Cu(111) substrate held at 180 K, and the sample was transferred into the low-temperature STM immediately after deposition. The residence time was counted by computer as the time between two abrupt current changes. Then the residence time was sorted, and the events with residence time longer than a certain value were counted by humans for exponential decay fit. The jumping events per unit time were counted by humans and divided by measuring time. DFT calculations were performed within the projector-augmented wave (PAW) plane wave approach, as implemented in the VASP code.[33−35] The exchange−correlation functional was treated with the generalized gradient approximation in the Perdew−Burke−Ernzerhof (PBE) form .[36] The simulated STM images were obtained in constant current mode within the Tersoff−Hamann approximation (*i.e.*, computing an iso-density surface $z(x,y)$ above the adsorbed molecule) .[37] For the comparison of the energies of the metastable states, the van der Waals interactions were included through a van der Waals density functional, as implemented in the GPAW code.[38,39] The simulation model contained the molecule on one copper layer. Only one copper layer was included due to the rather weak molecule-to-substrate interaction and due to the computational cost. Our test calculations confirmed that one layer is sufficient for these studies.[40]

Acknowledgment. This work was supported in part by the HKUST grant no. RPC07/08.SC02, the Hong Kong RGC grant no. CityU 102408, and the City U Centre for Applied Computing and Interactive Media. C.M. is grateful to the French Consulate General in Hong Kong and Macau for financial support.

REFERENCES AND NOTES

1. Balzani, V.; Credi, A.; Venturi, M. *Molecular Devices and Machines: A Journey into the Nanoworld*; Wiley-VCH: Weinheim, Germany, 2004.
2. *Molecular Switches*; Feringa, B. L., Ed.; Wiley-VCH: Weinheim, Germany, 2001.
3. van Delden, R. A.; ter Wiel, M. K. J.; Pollard, M. M.; Vicario, J.; Koumura, N.; Feringa, B. L. Unidirectional Molecular Motor on a Gold Surface. *Nature* **2005**, *437*, 1337–1340.
4. Joachim, C; Gimzewski, J. K. Single Nolecular Rotor at the Nanoscale. In *Molecular Machines and Motors*; Sauvage, J.-P., Ed.; Springer: Berlin, Germany, 2001; pp 1−18.
5. Kottas, G. S.; Clarke, L. I.; Horinek, D.; Michl, J. Artificial Molecular Rotors. *Chem. Rev.* **2005**, *105*, 1281–1376.
6. Carroll, R. L.; Gorman, C. B. The Genesis of Molecular Electronics. *Angew. Chem., Int. Ed.* **2002**, *41*, 4378–4400.
7. Ho, W. Single-Molecule Chemistry. *J. Chem. Phys.* **2002**, *117*, 11033–11061.
8. Pejov, L.; Rosa, M. L.; Kocarev, L. Dynamics of the Central Phenylene Ring Torsional Motion in Halogenated Phenylene Ethynylene Oligomers: A Quantum-Theoretical Contribution to the Study of Conformational Basis for Single-Molecule Switching Phenomena. *Chem. Phys.* **2007**, *340*, 1–11.
9. Heath, J. R. Molecular Electronics. *Annu. Rev. Mater. Res.* **2009**, *39*, 1–23.
10. Grill, L. Functionalized Molecules Studied by STM: Motion, Switching and Reactivity. *J. Phys.: Condens. Matter* **2008**, *20*, 053001(19 pp).
11. van Houselt, A.; Zandvliet, H. J. W. Time-Resolved Scanning Tunneling Microscopy. *Rev. Mod. Phys.* **2010**, *82*, 1593–1605.
12. Stipe, B. C.; Rezaei, M. A.; Ho, W. Inducing and Viewing the Rotational Motion of a Single Molecule. *Science* **1998**, *279*, 1907–1909.
13. Stipe, B. C.; Rezaei, M. A.; Ho, W. Coupling of Vibrational Excitation to the Rotational Motion of a Single Adsorbed Molecule. *Phys. Rev. Lett.* **1998**, *81*, 1263–1266.
14. Lastapis, M.; Martin, M.; Riedel, D.; Hellner, L.; Comtet, G.; Dujardin, G. Picometer-Scale Electronic Control of Molecular Dynamics Inside a Single Molecule. *Science* **2005**, *308*, 1000–1003.
15. Sainoo, Y.; Kim, Y.; Okawa, T.; Komeda, T.; Shigekawa, H.; Kawai, M. Excitation of Molecular Vibrational Modes with Inelastic Scanning Tunneling Microscopy Processes: Examination through Action Spectra of *cis*-2-Butene on Pd(110). *Phys. Rev. Let.* **2005**, *95*, 246102.
16. Hersam, M. C.; Guisinger, N. P.; Lyding, J. W. Isolating, Imaging, and Electrically Characterizing Individual Organic Molecules on the Si(100) Surface with the Scanning Tunneling Microscope. *J. Vac. Sci. Technol., A* **2000**, *18*, 1349–1353.
17. Iancu, V.; Hla, S.-W. Realization of a Four-Step Molecular Switch in Scanning Tunneling Microscope Manipulation of Single Chlorophyll-A Molecules. *Proc. Natl. Acad. Sci. U.S.A.* **2006**, *103*, 13718–13721.

18. Stohr, M.; Wagner, T.; Gabriel, M.; Weyers, B.; Moller, R. Direct Observation of Hindered Eccentric Rotation of an Individual Molecule: Cu-Phthalocyanine on C_{60}. *Phys. Rev. B: Condens. Matter Mater. Phys.* **2001**, *65*, 033404.
19. Vaughan, O. P. H.; Williams, F. J.; Bampos, N.; Lambert, R. M. A Chemically Switchable Molecular Pinwheel. *Angew. Chem., Int. Ed.* **2006**, *45*, 3779–3781.
20. Wintjes, N.; Bonifazi, D.; Cheng, F.; Kiebele, A.; Stohr, M.; Jung, T.; Spillmann, H.; Diederich, F. A Supramolecular Multiposition Rotary Device. *Angew. Chem., Int. Ed.* **2007**, *46*, 4089–4092.
21. Ye, T.; Takami, T.; Wang, R.; Jiang, J.; Weiss, P. S. Tuning Interactions between Ligands in Self-Assembled Double-Decker Phthalocyanine Arrays. *J. Am. Chem. Soc.* **2006**, *128*, 10984–10985.
22. Otsuki, J.; Komatsu, Y.; Kobayashi, D.; Asakawa, M.; Miyake, K. Rotational Libration of a Double-Decker Porphyrin Visualized. *J. Am. Chem. Soc.* **2010**, *132*, 6870–6871.
23. Baber, A. E.; Tierney, H. L.; Sykes, E. C. H. A Quantitative Single-Molecule Study of Thioether Molecular Rotors. *ACS Nano* **2008**, *2*, 2385–2391.
24. Gao, L.; Liu, Q.; Zhang, Y. Y.; Jiang, N.; Zhang, H. G.; Cheng, Z. H.; Qiu, W. F.; Du, S. X.; Liu, Y. Q.; Hofer, W. A.; et al. Constructing an Array of Anchored Single-Molecule Rotors on Gold Surfaces. *Phys. Rev. Lett.* **2008**, *101*, 197209.
25. Gimzewski, J. K.; Joachim, C.; Schlittler, R. R.; Langlais, V.; Tang, H.; Johannsen, I. Rotation of a Single Molecule within a Supramolecular Bearing. *Science* **1998**, *281*, 531–533.
26. Tabe, Y.; Yokoyama, H. Coherent Collective Precession of Molecular Rotors with Chiral Propellers. *Nat. Mater.* **2003**, *2*, 806–809.
27. Pascual, J. I.; Lorente, N.; Song, Z.; Conrad, H.; Rust, H.-P. Selectivity in Vibrationally Mediated Single-Molecule Chemistry. *Nature* **2003**, *423*, 525–528.
28. Grill, L.; Rieder, K.-H.; Moresco, F.; Rapenne, G.; Stojkovic, S.; Bouju, X.; Joachim, C. Rolling a Single Molecular Wheel at the Atomic Scale. *Nat. Nanotechnol.* **2007**, *2*, 95–98.
29. Chiaravalloti, F.; Gross, L.; Rieder, K.-H.; Stojkovic, S. M.; Gourdon, A.; Joachim, C.; Moresco, F. A Rack-and-Pinion Device at the Molecular Scale. *Nat. Mater.* **2007**, *6*, 30–33.
30. Moresco, F.; Meyer, G.; Rieder, K.-H.; Tang, H.; Gourdon, A.; Joachim, C. Conformational Changes of Single Molecules Induced by Scanning Tunneling Microscopy Manipulation: A Route to Molecular Switching. *Phys. Rev. Lett.* **2001**, *86*, 672–675.
31. Zheng, X.; Mulcahy, M. E.; Horinek, D.; Galeotti, F.; Magnera, T. F.; Michl, J. Dipolar and Nonpolar Altitudinal Molecular Rotors Mounted on an Au(111) Surface. *J. Am. Chem. Soc.* **2004**, *126*, 4540–4542.
32. Barigelletti, F.; Flamigni, L.; Balzani, V.; Collin, J.-P.; Sauvage, J.-P.; Sour, A. Luminescence Properties of Rigid, Rod-Like, Dichromophoric Species. Dinuclear Ru-Os Terpyridine-Type Complexes with 2.4 nm Metal-to-Metal Distance. *New. J. Chem.* **1995**, *19*, 793–798.
33. Blöchl, P. E. Projector Augmented-Wave Method. *Phys. Rev. B: Condens. Matter Mater. Phys.* **1994**, *50*, 17953–17979.
34. Kresse, G.; Joubert, J. From Ultrasoft Pseudopotentials to the Projector Augmented-Wave Method. *Phys. Rev. B: Condens. Matter Mater. Phys.* **1999**, *59*, 1758–1775.
35. Kresse, G.; Furthmüller, J. Efficiency of Ab-Initio Total Energy Calculations for Metals and Semiconductors Using a Plane-Wave Basis Set. *Comput. Mater. Sci.* **1996**, *6*, 15–50.
36. Perdew, J. P.; Burke, K.; Ernzerhof, M. Generalized Gradient Approximation Made Simple. *Phys. Rev. Lett.* **1996**, *77*, 3865–3868.
37. Tersoff, J.; Hamann, D. R. Theory of the Scanning Tunneling Microscope. *Phys. Rev. B: Condens. Matter Mater. Phys.* **1985**, *31*, 805–813.
38. Dion, M.; Rydberg, H.; Schröder, E.; Langreth, D. C.; Lundqvist, B. I. Van der. Waals Density Functional for General Geometries. *Phys. Rev. Lett.* **2004**, *92*, 246401.
39. Mortensen, J. J.; Hansen, L. B.; Jacobsen, K. W. Real-Space Grid Implementation of the Projector Augmented Wave Method. *Phys. Rev. B: Condens. Matter Mater. Phys.* **2005**, *71*, 035109.
40. Shi, X.; Zhang, R. Q.; Minot, C.;. Hermann, K.; Van Hove M.; Wang, W.; Lin. N. in preparation.